ISSN 1615-9306 · JSSCCJ 43 (8) 1393–1614 (2020) · Vol. 43 · No. 8 · April 2020 · D 10609

JSS

JOURNAL OF SEPARATION SCIENCE

8|20

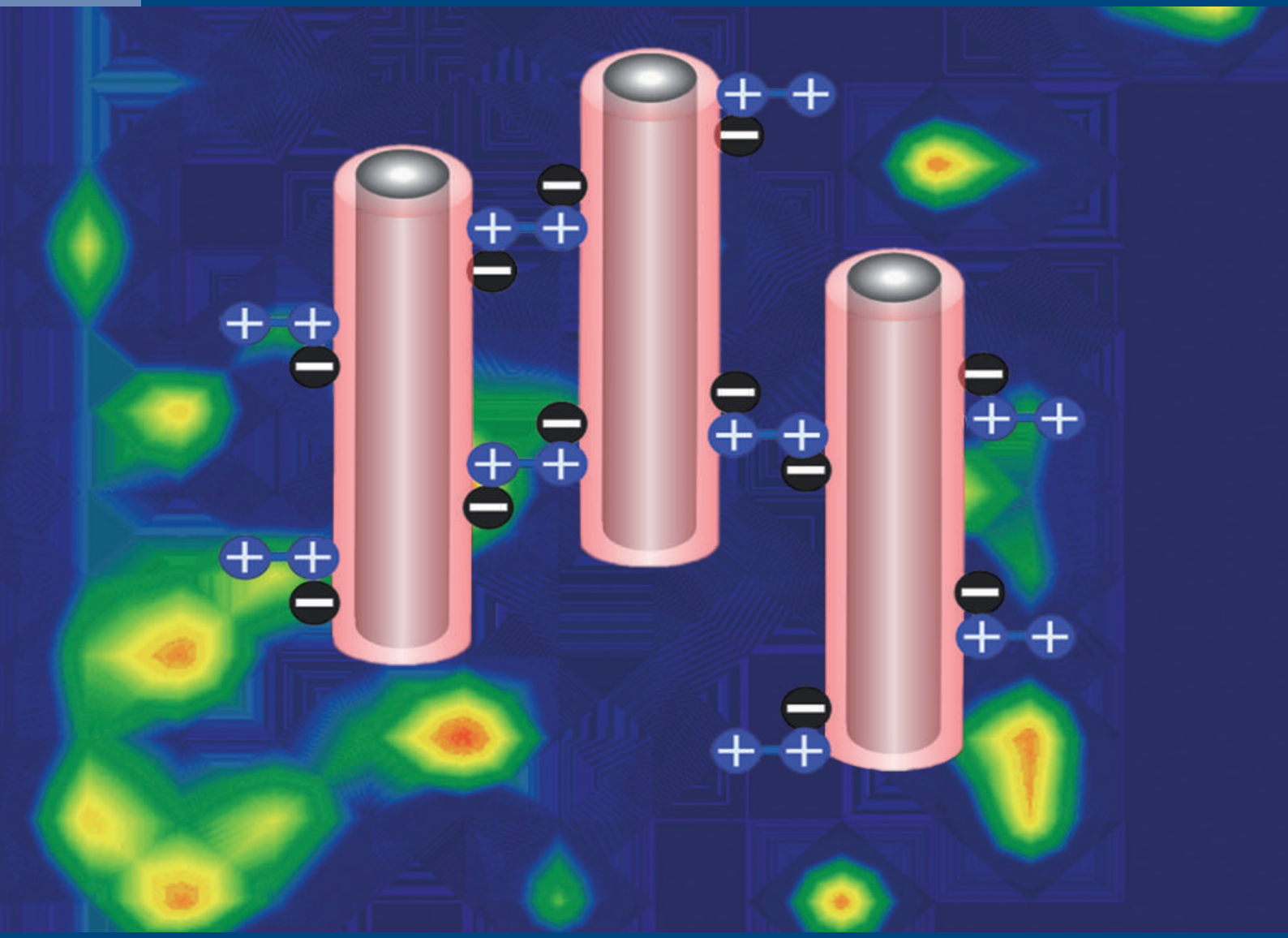

Methods
Chromatography · Electroseparation

Applications
Biomedicine · Foods · Environment

www.jss-journal.com

WILEY-VCH

Received: 20 November 2019 | Revised: 4 February 2020 | Accepted: 7 February 2020

DOI: 10.1002/jssc.201901178

RESEARCH ARTICLE

JOURNAL OF SEPARATION SCIENCE

Computational and experimental validation of free radical scavenging properties of high-performance thin-layer chromatography quantified phenyl myristate in *Homalium nepalense*

Satish Kanhar[1] | **Partha Pratim Roy**[2] | **Atish Kumar Sahoo**[1]

[1]Medicinal & Aromatic Plant Division, Regional Plant Resource Centre, Forest & Environment Department, Government of Odisha, Bhubaneswar, India

[2]Division of Pharmaceutical & Medicinal Chemistry, Institute of Pharmacy, Guru Ghasidas University, Bilaspur, Chhattisgarh, India

Correspondence
Dr. Atish Kumar Sahoo, Senior Scientist, Medicinal & Aromatic plant division, Regional Plant Resource Centre, Forest & Environment Department, Govt. of Odisha, Nayapalli, Bhubaneswar-751015, India.
Email: atish_kumar1976@yahoo.co.in

Funding information
National Medicinal Plant Board (NMPB), Department of AYUSH, Govt. of India, New Delhi, Grant/Award Number: Z.18017/87/CSC/R&D/OR-01/2013-14-NMPB

Phenyl myristate was isolated from *Homalium nepalense*, which is known for its therapeutic virtues in traditional medicine. However, the study of radical scavenging-capacity of phenyl myristate is limited by its relatively low abundance in medicinal plants. We have studied the isolation, structure-elucidation, and bioactivities of high-performance thin-layer chromatography validated phenyl myristate from hydroalcohol-extract of bark of *H. nepalense*. The chemical structure of phenyl myristate was elucidated by spectroscopic methods. The chromatography was performed on high-performance thin-layer chromatography aluminum plates coated with silica-gel 60 F_{254}. Determination and quantitation of phenyl myristate were performed by densitometric-scanning at 254 nm (chloroform-methanol, 9:1, v/v; R_f 0.49). The method was validated according to International Council for Harmonisation guidelines in terms of linearity, specificity, sensitivity, accuracy, precision, robustness, and stability. Linearity-range of phenyl myristate was 100–500 ng/5 μL with correlation-coefficient $r^2 = 0.9997$. Limits of detection and quantitation were 3.35 and 10.17 ng, respectively. Phenyl myristate showed significant free-radical-scavenging activities in 2,2-diphenyl-1-picrylhydrazyl, oxygen-radical-absorbance-capacity, and ex vivo cell-based-antioxidant-protection-in-erythrocytes assays. Molecular-docking approach of phenyl myristate showed effective binding at active sites of human serum albumin (HSA) with the lowest binding energy (−8.4 kcal/mol) that was comparable with ascorbic acid (−5.0 kcal/mol). These studies provide mechanistic insight into the potential free radical scavenging activities of phenyl myristate.

KEYWORDS
antioxidants, *Homalium nepalense*, molecular docking, phenyl myristate, thin-layer chromatography

1 | INTRODUCTION

Natural products-based drug discovery research is an integral part of lead findings against various pharmacological targets in life-threatening diseases. The advent of technologies in the pharmaceutical industries shifted their research from synthetic drug libraries to natural product drug discovery for the development of unique lead molecules to treat different

Article Related Abbreviations: AAPH, 2,2′-azobis (2-amidino-propane) dihydrochloride; CAP-e, cell-based antioxidant protection in erythrocytes; DCF-DA, 2′,7′-dichlorofluorescein diacetate; DPPH, 2,2-diphenyl-1-picrylhydrazyl; FL, Fluorescein; ICH, International Council for Harmonisation; ORAC, oxygen radical absorbance capacity; PDB, protein data bank; PM, phenyl myristate; QC, quality control; RSC, radical scavenging capacity.

 © 2020 WILEY-VCH Verlag GmbH & Co. KGaA, Weinheim

diseases. In recent, drug development is focused on the synergistic application of computational techniques, ethnopharmacological validation, bioassay-guided isolation, biosynthesis, plant biotechnology, and a wide range of bioactivity screening models [1,2].

Homalium nepalense (Wall) Benth. (Salicaceae) is a medicinal plant native to the state of Odisha and Andhra Pradesh, India. In traditional practices [3], leaf and bark are used for the treatment of wound healing [4], stomach disorder [5], puerperal fever [5,6], free radical scavenging, and hepatoprotective activities [7,8]. As this species possess diversified bioactive compounds; adulterations may cause variability in the active ingredients and influence the efficacy and safety of the drug. In recent years, high-performance thin-layer chromatography (HPTLC) emerged as a sophisticated analytical tool in quality control of complex plant matrices due to its low operating cost, less analysis time, high sample throughput, and simultaneous determination of several compounds at nanogram level [9,10]. It also enables to detect compounds having no UV absorption by post derivatization HPTLC [11].

The study highlights the isolation, structural elucidation, and quantification of phenyl myristate (PM) in *H. nepalense*. Extensive literature survey revealed that there are no validated HPTLC methods available for quantification of PM. To the best of our knowledge, no study concerning the bioactivities of PM has been reported. 2,2-Diphenyl-1-picrylhydrazyl (DPPH), oxygen-radical absorbance-capacity (ORAC), and ex vivo cell-based-antioxidant-protection-in-erythrocytes (CAP-e) assays were performed. Computational molecular docking analysis was carried out to get insight into the binding interactions of the ligands (PM) and oxidative stress-related protein (human serum albumin, HSA). ORAC assay was performed to quantify the antioxidant capacity of the drug towards different oxidants e.g. hydroxyl radicals, peroxyl radicals, and peroxynitrite. CAP-e assay was performed on RBCs as it does not produce ROS and undergo apoptosis. To our knowledge, this is the first report demonstrating the free radical scavenging activities of PM.

2 | MATERIALS AND METHODS

2.1 | Chemicals and reagents

All chemicals (analytical grade) and solvents (HPLC grade) were purchased from SISCO Research Laboratories Mumbai, India, Himedia Laboratories, India, and Merck India, Mumbai, India.

2.2 | Plant material

Bark and leaves of *Homalium nepalense* (Wall) Benth. (Salicaceae) were collected from Banei forest, Sundergarh, Odisha, India. The species was identified and authenticated by Dr. P. C. Panda, Taxonomist, Regional Plant Resource Centre, Bhubaneswar, India and deposited at our Centre for future reference (2391/RPRC).

2.3 | Extraction and isolation

Fresh leaves and barks were air dried at room temperature (25–30°C) and grounded to powder material. Dried materials (bark and leaf, each 700 g) were defatted with 2.5 L petroleum ether for 24 h and chlorophyll was removed by chloroform (2.5 L, 24 h). Then, both extracted materials were treated with 70% hydroalcohol (2.5 × 2 L, 72 h) by maceration in percolator and filtered. The filtrate was evaporated under reduced pressure in rotary evaporator (R-100, Buchi, Switzerland) to obtain semisolid mass of hydroalcohol extract of bark (HNHB; 28.16% w/w) and leaf (HNHL; 23.32% w/w). The HNHB (180 g) was subjected to silica gel (100–200, mesh) column chromatography (Borosil, 100 × 5 cm) and eluted successively by gradient elution method using hexane (100%) to obtain 30 fractions (F_1–F_{30}, 10 mL each) and hexane–chloroform (95:5–0:100, v/v) to get 200 fractions (F_{31}–F_{230}, 10 mL each). The eluted fractions (F_{161}–F_{170}) from hexane–chloroform (30:70, v/v, 10 mL each) were pooled into a single fraction on the basis of same R_f values (0.49; chloroform–methanol, 9:1, v/v), and then dried, purified, and recrystallized with methanol to obtain yellowish-white powder (PM, 21.8 mg, 0.0121% with respect to HNHB). The purity was cross-checked by TLC with a brown colored single spot visualized at 254 nm (R_f 0.49, chloroform-methanol, 9:1, v/v) and the melting point was recorded.

2.4 | Spectroscopic analysis of isolated compound PM

Melting point (MP, ºC) was determined in capillaries by using melting point apparatus (SMP-30, Stuart, UK). UV absorbance was recorded at scanning wavelength (200–800 nm) by UV–Vis spectrophotometer (UV 1800, Shimadzu, Japan). IR spectrum was recorded on KBr pellets by FTIR spectrometer (JASCO 410, Tokyo, Japan). MS spectrum (Agilent 6520 Q-TOF, US) was obtained in ESI (positive mode). NMR spectra were recorded by Bruker AvIII HD-300 MHz (US) operating at 300 MHz (^{1}H) and 75 MHz (^{13}C) in $CDCl_3$ with TMS as internal standard and chemical shifts were reported in δ units.

2.5 | High-performance TLC validation of PM

2.5.1 | Instrumentation

Aluminum foil backed HPTLC silica gel 60 F_{254} (10 × 10 cm, 250 mm thickness, Merck, Germany) plates were used as a stationary phase. Samples (PM, HNHL, and HNHB) were sprayed on HPTLC plate with Hamilton syringe sample applicator (Linomat 5, CAMAG, Switzerland) under nitrogen gas

flow and dried on a hot plate (TLC Plate Heater 3, CAMAG, Switzerland). Chromatograms were developed in twin trough chambers (20 × 10 cm, CAMAG, Switzerland) and densitometry analysis was carried out by CAMAG TLC Scanner 3, fitted with winCATS Planar Chromatography Manager (version 1.14.26, CAMAG, Switzerland).

2.5.2 | Chromatographic condition

Samples were dissolved in methanol (5 μL) and applied on HPTLC plate by using sample applicator (150 nL/s) as bands (length 6 mm, distance 25 mm) at 10 mm distance from each side and bottom of the plates. HPTLC plates developed in twin trough chamber (chloroform–methanol; 9:1, v/v, 10 mL) to a distance of 90 mm. Detection and densitometric scanning were performed by CAMAG TLC Scanner 3 in absorption mode at 254 nm with the slit dimension (6 × 0.3 mm). Sample track scanning speed was 20 mm/s and it was performed under control of winCATS Planar Chromatographic Manager.

2.5.3 | Preparation of solutions

Standard stock solution of PM (100–500 μg/μL) and each sample of HNHL and HNHB were prepared in HPLC grade methanol (1 mg/mL) [12].

2.5.4 | Method validation

HPTLC method was validated according to International Council for Harmonisation (ICH) guidelines for linearity, specificity, sensitivity, accuracy, precision, robustness, and stability [10].

2.5.5 | Linearity

Linearity was ascertained by using different concentrations of PM (100–500 ng/5 μL) in triplicate. SD, coefficient of determination (r^2), slope, and intercept of calibration curves were estimated to determine linearity. The peak area versus concentration was plotted to determine regression equation ($y = mx + c$) and r^2 [13].

2.5.6 | Specificity

To verify the specificity method, PM (100 ng/5 μL) and each sample of HNHL and HNHB (500 ng/5 μL) were applied on HPTLC plate, developed, and scanned. The specificity of the experiment was established by comparing retention factor (R_f), start and end position of PM with samples [12,13].

2.5.7 | Sensitivity

The sensitivity of the method was determined as LOD and LOQ by applying PM (100–500 ng/5 μL). LOD and LOQ were calculated based on SD (σ) and slope (S) of the calibration curve in triplicates.

$LOD = 3.3 \times \sigma/S$ and $LOQ = 10 \times \sigma/S$ (σ = SD of intercept and S = slope of calibration plot) [12,13].

2.5.8 | Accuracy

Accuracy was determined by calculating recovery of PM in samples by standard addition method. PM was spiked to 50, 100, and 150% of prequantified sample (500 ng/5 μL) and their peak area and percentage recoveries were calculated in triplicates [12,13].

2.5.9 | Precision

Precision was determined as intraday (repeatability) and interday (reproducibility) method. Intraday precision of PM (100–500 ng/5 μL) was measured on the same day in triplicate. Interday precision of PM of same concentrations was measured as triplicate for two consecutive days. Results were expressed as %RSD [12, 13].

2.5.10 | Robustness

Robustness was performed by varying mobile phase composition (chloroform–methanol, 8.8:1.2, 9:1, and 9.2:0.8, v/v), mobile phase volume (10 ± 5 mL), elution length (90 ± 5 mm), saturation time (10 ± 5 min), and time of TLC development to scanning (10 ± 5 min) for PM (100 ng/5 μL). Results were expressed as %RSD [12,13].

2.5.11 | Stability

Stability was determined by applying PM (100 ng/5 μL) on HPTLC plate and the developed plates were scanned at different interval of 0, 2, 4, 6, and 8 h, respectively. Peak areas of PM at different time intervals were calculated and expressed as %RSD [14].

2.6 | Free radical scavenging studies

2.6.1 | 2,2-Diphenyl-1-picrylhydrazyl assay of PM

Free radical scavenging potential of PM, HNHB, and HNHL were assessed by DPPH assay. DPPH (0.1 mM, 1 mL) was mixed with each sample (PM, HNHB, and HNHL, 1 mg/mL, 2 mL) and kept for 20 min in dark. After incubation, absorbance was measured at 517 nm in microplate reader (Synergy H1MF, BioTek, USA). Ascorbic acid was used as the standard drug and results were expressed as IC_{50} (μg/mL) [7].

2.7 | Oxygen-radical absorbance-capacity assay of PM

ORAC assay was performed by following the method [8]. Fluorescein (FL, 78 nM, 50 μL) and PM (50 μL) were taken in a microplate and incubated at 37°C for 15 min (Synergy H1MF,

BioTek, USA). Then, AAPH (221 mM, 25 μL) was added and fluorescence was recorded (excitation 485 nm and emission 520 nm) at 1 min interval for 30 min in a microplate reader (Synergy H1MF, BioTek, USA). The net area under the curve (AUC) was calculated by subtracting the AUC of antioxidant with AUC of blank. Trolox (20 μM) was used as standard drug.

$$\text{AUC for standard/PM} = \left(0.5 + F_1/F_0 + F_2/F_0 + \cdots\cdots\cdots .F_n/F_0\right) \times 5 \quad (1)$$

2.8 | Cell-based-antioxidant-protection-in-erythrocytes assay of PM

CAP-e assay was performed with the approval of the Institutional Animal Ethics Committee (Regd. No. 1807/GO/R/S/15/CPCSEA) of the Centre, and conducted according to the guidelines of the CPCSEA, New Delhi, India [8]. One milligram of each PM, HNHB, and HNHL was mixed with 0.9% saline (5 mL) at physiological pH. RBCs (Wistar albino rats) were washed twice in physiological saline and treated with different dilutions of PM, HNHB, and HNHL. RBCs untreated with test samples were considered as negative control, whereas RBCs with standard oxidizing agent were considered as positive control. Oxidative damage was initiated by adding AAPH and the degree of oxidant damage was recorded with the decrease in fluorescence intensity (FI) of 2,7-dichlorofluorescein diacetate (DCF-DA) dye, by measuring in a microplate reader (Synergy H1MF, BioTek, USA). Trolox was taken as a reference drug and IC_{50} of PM, HNHB, and HNHL were calculated (μg/mL).

$$FI = \left(FI_{max} - FI_{sample}\right)/\left(FI_{sample} - FI_{untreated}\right) \quad (2)$$

2.9 | Molecular docking studies of PM

AutoDock Vina (version 1.1.2) was used to predict the ligand–protein binding mode interaction. Receptor structure (human serum albumin, HSA; PDBID: 2BXK) was retrieved from protein data bank (PDB). The protein optimization for docking was performed by removing all water molecules and polar hydrogen atoms were added to the refined model using AutoDock Vina (version 1.1.2). MGL tool software was used to generate PDBQT, partial charge (Q), and atom type (T) files and its 3D visualization. The structure of ascorbic acid was retrieved from PubChem while structure of PM was constructed in 2D and converted to 3D by using ChemDraw (Ultra 8.0.3). Further, energy minimization was performed through MM2 force field (RMSD = 0.001, maximum number of steps = 10 000 using conjugate gradient method) and Hartree-Fock method (3–21 as basis set) using GAMESS (version 12.0) to obtain the initial conformation of PM. The grid with a grid space (1 and 28 Å) in each of the x, y, and z dimension was prepared around the active site of the receptor (binding site of the co-crystallized ligand indomethacin). The docking complex stability was measured on the basis of interaction energy [15,16].

2.10 | Statistical analysis

Analysis of analytes was performed in triplicate. Results were expressed as mean ± SD. Statistical comparison of results was performed at $P < 0.05$ by one-way analysis of variance (one-way ANOVA) followed by Dunnett's multiple comparison test using GraphPad software (Prism 7).

3 | RESULTS AND DISCUSSION

3.1 | Structural elucidation of PM

The isolated compound PM was obtained as yellowish-white powder (21.8 mg, 0.0121% with respect to HNHB). The purity was cross-checked by TLC with a brown colored single spot visualized at 254 nm (R_f 0.49, chloroform–methanol, 9:1, v/v) and the melting point was recorded at 78–79°C (Figure 1A). UV spectrum with absorbance maxima was recorded (CH_3OH), λ_{max} at 254 nm indicated the presence of C_6H_5 group in the structure (Figure 1C). IR spectrum showed absorption at 1228 ($C–O_{stretch}$), 1463.72 ($C=C_{stretch}$), 1698.67 (aromatic $C–H_{stretch}$), and 2916.48 cm^{-1} ($C=O_{stretch}$). Molecular mass was determined by ESI–HRMS (positive mode) and showed molecular ion peak at *m/z* 305.17 $[M+H]^+$ with base peak at *m/z* 212.0193 [$C_{14}H_{27}O$, 100%]$^+$. Other intense mass fragmentation ion peaks appeared at *m/z* 197.18 $[C_{13}H_{24}O]^+$, 183.17 $[C_{12}H_{22}O]^+$, 169.15 $[C_{11}H_{20}O]^+$, 155.14 $[C_{10}H_{18}O]^+$, 141.12 $[C_9H_{16}O]^+$, 127.1 $[C_8H_{14}O]^+$, 113.09 $[C_7H_{12}O]^+$, 99.07 $[C_6H_{10}O]^+$, 85.06 $[C_5H_8O]^+$, 71.04 $[C_4H_6O]^+$, 57.03 $[C_3H_4O]^+$, and 43.01 $[C_2H_2O]^+$ (Figure 1B). ^{1}H-NMR spectrum of PM was analyzed by the aid of heteronuclear multiple-bond correlation spectroscopy (HMBC). Signals for methyl protons appeared as singlet at δ_H 0.89 (H-1, s). The characteristic signals for methylene protons showed at δ_H 1.18–1.54 and aromatic protons signals at δ_H 7.20–7.28. ^{13}C-NMR spectrum showed signal for methyl carbon at δ_C 14.1 and methylene carbon signals appeared at δ_C 29.1–33.5. Carbonyl carbon showed characteristics signal at δ_C 172.3; whereas aromatic carbon signals appeared at δ_C 121.5–151.4. A critical observation of the HMBC correlation between aromatic proton H-2′ and H-6′ (δ_H 7.20) with C-14 (δ_C 172.3) revealed the presence of carbonyl group (C=O) in PM (Supporting Information Table S1). Based on spectroscopic data, isolated compound was identified as PM or phenyl tetradecanoate (Figure 1A) and reported first in *H. nepalense*.

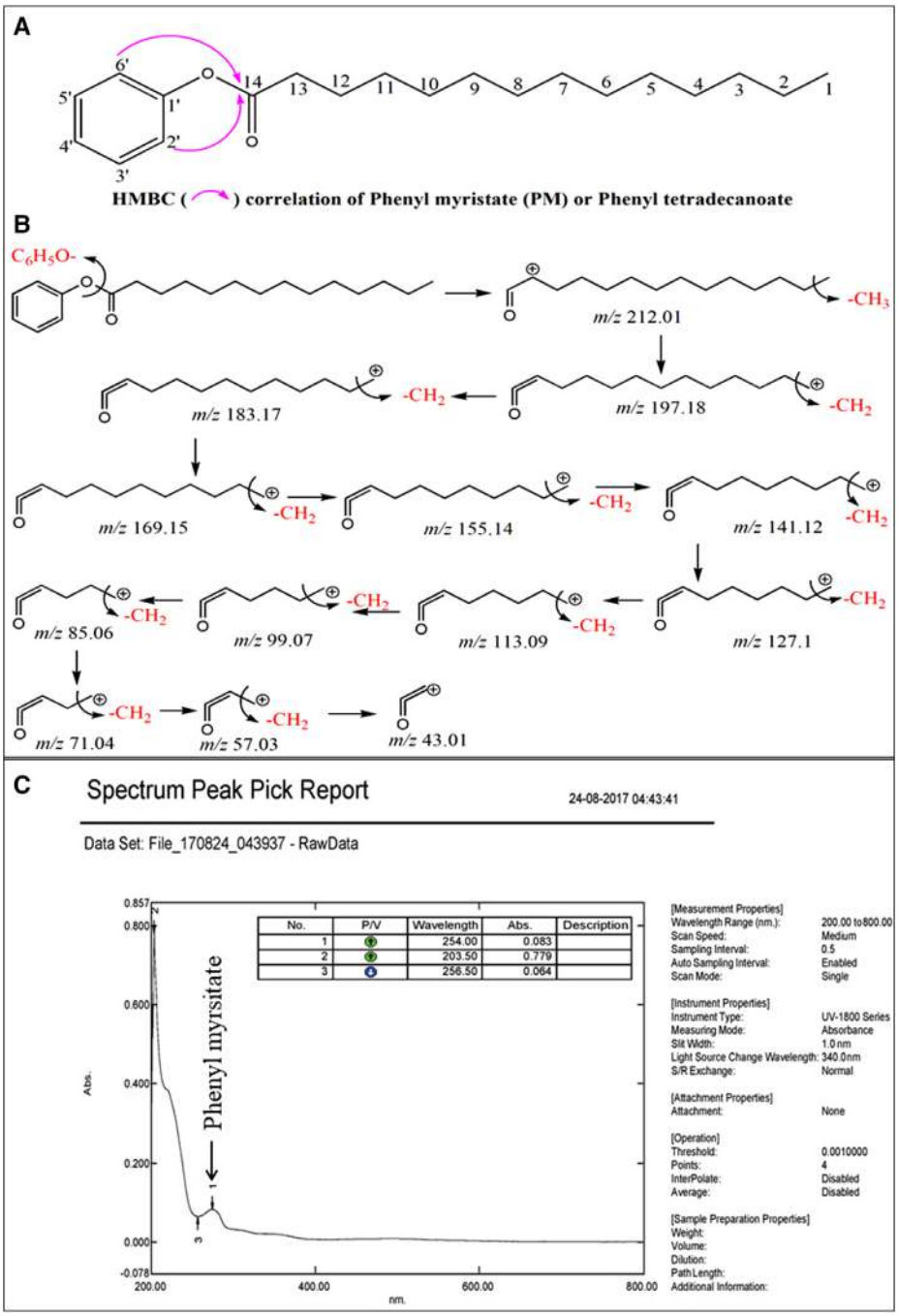

FIGURE 1 (A) Structure of PM. (B) Mass fragmentation pattern of PM. (C) UV absorption spectrum of PM (500 μg/mL) scanned at 200–800 nm and absorbance maxima (λ_{max}) of PM and solvent (MeOH) recorded at 254 nm and 203 nm respectively

3.2 | HPTLC study of PM

3.2.1 | Optimization of chromatographic conditions

The improved separation and resolution of bands of PM, HNHL, and HNHB on HPTLC plates were obtained (chloroform–methanol; 9:1, v/v). HPTLC fingerprint patterns were quantitated accurately by recording R_f value (0.49) of isolated drug PM at absorbance maxima of 254 nm (Figure 2A, B, and D–F). From the chromatographic patterns, PM was passed the chemical test and validated by HPTLC (Supporting Information Table S2).

3.2.2 | Linearity

Linearity was performed by using different concentrations of PM (100–500 ng/5 μL) and calibration curve was plotted between peak areas and concentrations. Under optimized conditions, linear regression analysis displayed good linear

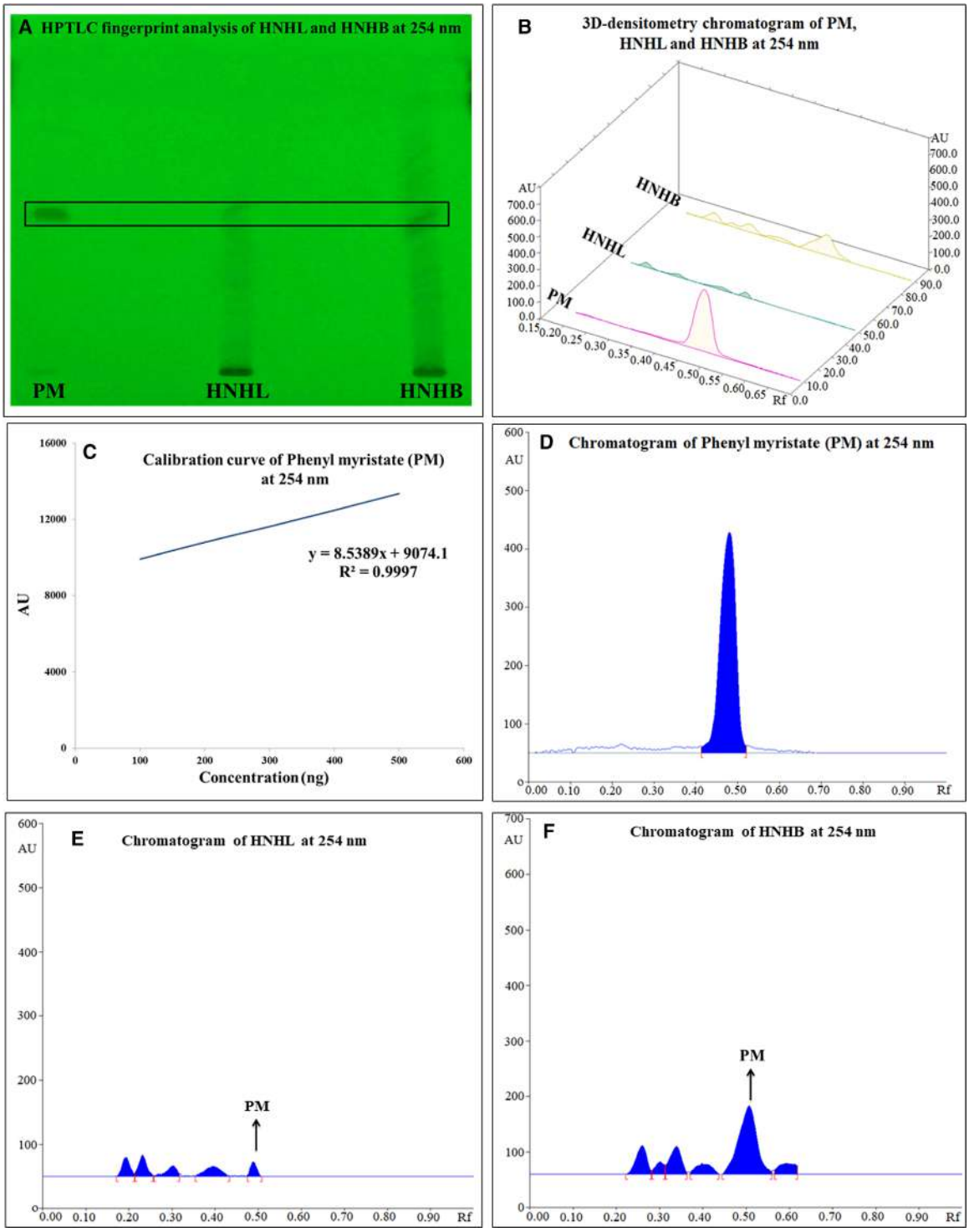

FIGURE 2 (A) HPTLC fingerprint analysis of HNHL and HNHB at 254 nm. (B) 3D Densitometric chromatogram of PM, HNHL, and HNHB at 254 nm. (C) Calibration curve of PM. (D) HPTLC chromatogram of PM at 254 nm. (E and F) HPTLC chromatogram of HNHL and HNHB at 254 nm respectively. HNHB-*H. nepalense* hydroalcohol extract of bark, HNHL-*H. nepalense* hydroalcohol extract of leaf

relationship with respect to concentration and peak area of PM (Figure 2C).

3.2.3 | Specificity

Specificity was investigated by analyzing the chromatograms of HNHL and HNHB at peak start, middle, and at peak end under optimized conditions. The peak of R_f 0.49 was matched exactly with the corresponding R_f 0.49 of PM at 254 nm (Figure 2A). The results showed that there were no interfering bands and impurity within same R_f values of HNHL and HNHB, thus the method was found to be specific (Figure 2A and B).

3.2.4 | Sensitivity

Sensitivity of the study was expressed as LOD and LOQ. LOD and LOQ were calculated by SD and slope of calibration curve of PM (Figure 2C) and were found to be 3.35 and 10.17 ng/5 μL at 254 nm, respectively. Thus, the method was sufficiently sensitive for a precise determination at nanogram level (Supporting Information Table S2).

3.2.5 | Accuracy

Accuracy was calculated by recovery studies and validated by standard addition of PM at three different concentrations (50, 100, and 150 ng) in HNHL and HNHB. The average recoveries were found to be 90.14 and 95.61% in HNHL and HNHB, respectively, and the results indicate that the proposed method was accurate (Supporting Information Table S3).

3.2.6 | Precision

Precision was determined by measuring intraday (1 day) and interday (two consecutive days) variation in peak area and %RSD were calculated. The values of %RSD of PM at five different concentrations (100–500 ng/5 μL) were found to be <1 for intraday (0.011–0.015) and interday (0.013–0.018) at 254 nm confirmed the precision of the method (Supporting Information Table S3).

3.2.7 | Robustness

Robustness was achieved with the composition (chloroform–methanol; 8.8:1.2, 9:1, and 9.2:0.8, v/v), volume (10 ± 5 mL), and elution length (90 ± 5 mm). The optimized time for TLC chamber saturation and TLC development to scanning was 10 ± 5 min. The robustness of PM was varied slightly through its R_f 0.49 ± 0.05 at 254 nm. The %RSD values for peak area were <1.0 indicated the highly robust nature of the developed method (Supporting Information Table S3).

3.2.8 | Stability

To determine stability of PM, chromatogram was developed at 0, 2, 4, 6, and 8 h and peak area was calculated at each time interval. At 0 h, mean peak area was found to be 9920.36 ± 1.244 whereas at 8 h, mean peak area was 9869.56 ± 1.524. Thus, the results indicated that PM was stable under typical processing and storage conditions of analytical procedure (Supporting Information Table S3).

3.3 | Free radical scavenging activities

3.3.1 | 2,2-Diphenyl-1-picrylhydrazyl activity of PM

Free radical scavenging activities of HNHB, HNHL, and PM were measured by the decrease in absorbance of DPPH solution at 517 nm. IC_{50} values of HNHB and HNHL were found to be 101.2 and 120.89 μg/mL, respectively; whereas the isolated drug PM was reported at 25.98 μg/mL and found comparable to the standard drug ascorbic acid (17.73 μg/mL; Figure 3A and B). Free radicals produced by DPPH were dose dependently and significantly ($P < 0.001$) inhibited by PM. The free radical scavenging activity was due to the binding of PM (at C-14) to DPPH radicals to form a stable product (2,2-diphenyl-1,1-tridecanyl picrylhydrazine; Figure 3C). The underlying reaction mechanism indicates single electron transfer (SET) mechanism of PM to neutralize DPPH free radical and thus, it may be explored as a therapeutic agent in free radical-induced diseases [17].

3.4 | Oxygen-radical absorbance-capacity assay of PM

Free radical scavenging potential in terms of fluorescence quenching effect of HNHB, HNHL, and PM were evaluated by ORAC assay. It is based on principle of inhibition of in situ generated peroxy free radical that is responsible for damaging fluorescent compound (fluorescein) with the decrease its fluorescent intensity (FI) and increase the rate of fluorescent decay. Net AUC of PM, HNHB, and HNHL were 54.35 ± 0.54, 42.3 ± 0.81, and 32.85 ± 0.66, respectively; whereas net AUC of trolox was 61.15 ± 0.69. PM was found to be comparable to trolox (Figure 3D). The underlying reaction mechanism is the step by step sequence of elementary reactions of PM towards the ability to scavenge peroxyl radical (generated by thermolysis of AAPH). On thermolysis of AAPH, amidinopropane radicals were formed and reacted with O_2 to form peroxy amidinopropane radicals, which were further reacted with fluorescein to exhibit maximum FI. However, PM (at C-14) react with peroxy amidinopropane radicals to form a stable product (tridecanyl amidinopropyl peroxide) and thus reduced the chemiluminescence intensity of fluorescein sodium (Figure 3F).

3.5 | Cell-based-antioxidant-protection-in-erythrocytes assay of PM

The cellular protection ability of PM, HNHB, and HNHL were measured to access the formation of peroxyl radicals generated inside and outside RBCs with the reaction of AAPH (peroxyl radical generator) and DCF-DA (fluorescent probe). IC_{50} values were found to be 41.61 ± 0.65, 82.37 ± 0.56, and 100.64 ± 1.26 μg/mL for PM, HNHB, and HNHL, respectively; whereas IC_{50} of trolox was 37.5 ± 0.67 μg/mL (Figure 3E). PM was found comparable with trolox. Ex vivo cellular mechanism to protect cell membranes and lipoproteins was based on the long alkyl chain of PM covalently or non-specifically adsorbed on RBC surface and scavenge the peroxy amidinopropane (generated from thermolysis of

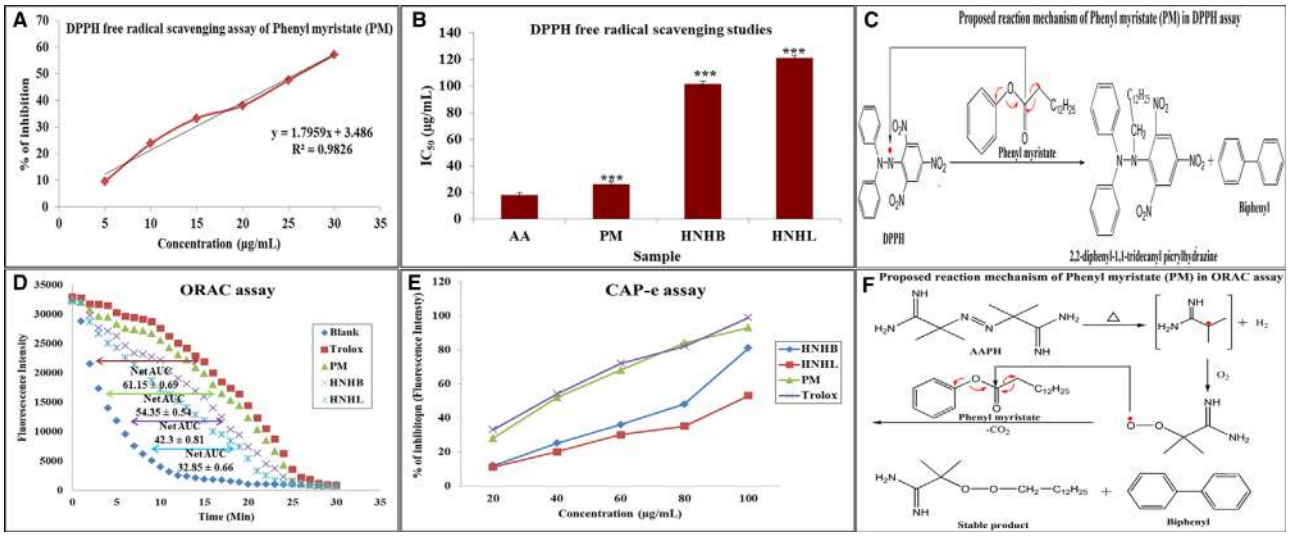

FIGURE 3 (A) DPPH free radical scavenging activity of PM and IC_{50} was found to be 25.98 µg/mL. (B) Comparative in vitro DPPH free radical scavenging studies of AA, PM, HNHB, and HNHL. Results were in triplicate and values were expressed as mean ± SD. *** Statistically significant difference between AA and samples (PM, HNHB, and HNHL) were performed at $P < 0.05$ by one-way analysis of variance (ANOVA) followed by Dunnett's post-test. (C) Represents proposed reaction mechanism of PM toward scavenging of DPPH free radical in which PM reacts with DPPH to form stable product (2,2-diphenyl-1,1-tridecanyl picrylhydrazine). (D) Represents area under curve (AUC) in oxygen radical absorbance capacity (ORAC) assay of HNHB, HNHL, and PM with net AUC 42.3 ± 0.81, 32.85 ± 0.66, and 54.35 ± 0.54, respectively, and were comparable to net AUC of standard drug trolox (61.15 ± 0.69). (E) Ex vivo cell-based antioxidant protection (CAP-e) assays of HNHB, HNHL, and PM with IC_{50} values 82.37 ± 0.56, 100.64 ± 1.26, and 41.61 ± 0.65 µg/mL, respectively, and were comparable to standard drug trolox (IC_{50} 37.5 ± 0.67 µg/mL). (F) represents proposed reaction mechanism of PM toward scavenging of peroxyamidino propane radicals generated by thermolysis of 2,2′-azobis-(2-amidino-propane)dihydrochloride (AAPH) in which PM reacts with peroxy amidinopropane radicals to form stable product (tridecanyl amidinopropyl peroxide). HNHB-*H. nepalense* hydroalcohol extract of bark, HNHL-*H. nepalense* hydroalcohol extract of leaf

AAPH) radicals to form stable product (tridecanyl amidinopropyl peroxide).

Oxidative stress is believed to play a role in diabetes, inflammation, hepatotoxicity, and neurodegenerative diseases. The previous report of free radical scavenging and hepatoprotective activities of *H. nepalense* is thus supported with result of the current investigation of PM made through DPPH, ORAC, and CAP-e assays [7,8]. Traditional uses of the bark of *H. nepalense* toward the treatment of oxidative stress-related wound healing and stomach and liver disorder may be justified through free radical scavenging studies [4,5,8]. It may, therefore, be claimed that the species contains important biological macromolecules such as PM, which is a free radical scavenger that contributes to hepatoprotective activities.

3.6 | Molecular docking studies of PM

Molecular docking studies were performed to investigate the potential interactions between this biological macromolecule PM and human serum albumin (HSA) active sites residues. The active site of HSA was surrounded by amino acid residues Leu 198, Leu 457, Glu 450, Phe 206, Leu 481, Leu 347, Ala 210, Phe 211, Trp 214, Ser 202, Arg 484, and Ser 454. The active site residues showed different tendencies to interact with PM and provide stability to complex by forming hydrogen bond, Van der Waals, and hydrophobic interactions. Binding pattern of ascorbic acid (magenta), PM (brown) to the co-crystallized ligand indomethacin (yellow) was evidenced (Figure 4). It is apparent that indomethacin bound with HSA by hydrogen bonding as well as hydrophobic interactions while ascorbic acid showed hydrogen bonding with HSA and PM bound to the active site (Phe 206, Leu 481, Leu 347, Ala 210, Phe 211, Trp 214, Ser 202, Arg 484, and Ser 454) of HSA by hydrophobic interactions owing to its long hydrocarbon chain (Figure 4). Further, a comparison of the binding energies of PM (−8.4 kcal/mol) and ascorbic acid (−5.0 kcal/mol) showed that PM have more affinity toward oxidative stress-related protein (HSA) than ascorbic acid and may be used as a potent antioxidant drug [16].

4 | CONCLUDING REMARKS

A new HPTLC densitometric method was developed for the analysis of PM in *H. nepalense* and validated according to ICH guidelines in terms of linearity, specificity, sensitivity, accuracy, precision, robustness, and stability. The procedure is simple, rapid and inexpensive in comparison with other analytical methods. The data could be used as a QC

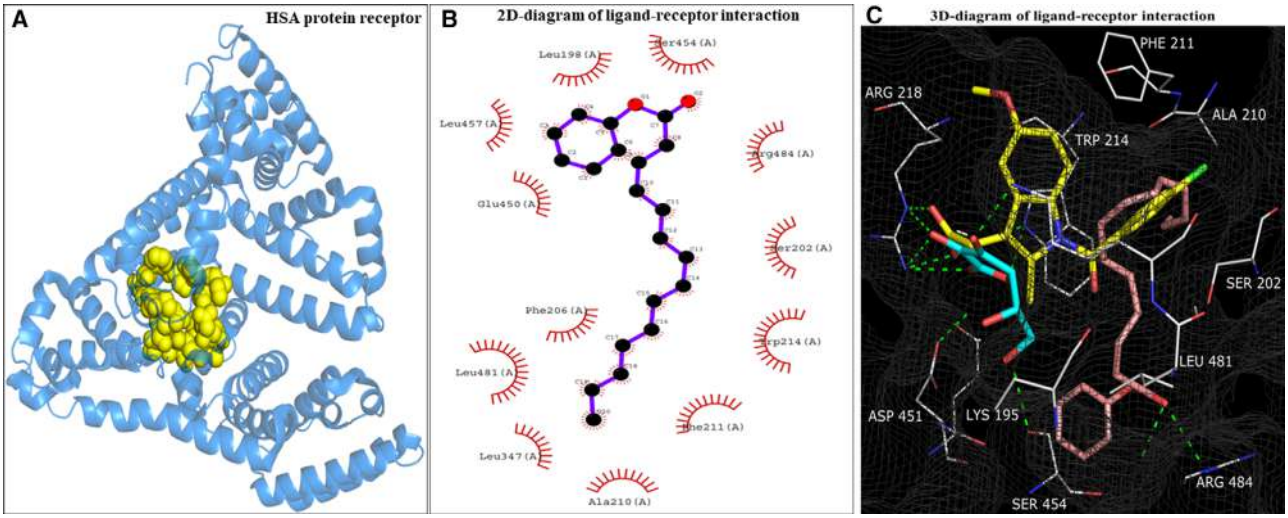

FIGURE 4 In silico molecular docking study of PM with human serum albumin (HSA). (A) Structure of HSA receptor protein. (B) 2D Diagram of ligand (PM)-receptor (HSA) interaction. (C) 3D Diagram of ligand (PM, ascorbic acid, indomethacin)-receptor (HSA) interaction. PM (brown), ascorbic acid (magenta), and indomethacin (yellow)

standard. In vitro (DPPH, ORAC) and ex vivo (CAP-e) studies concluded that PM is an important biological macromolecule in *H. nepalense* has free radical scavenging potential whereas the results of molecular docking analysis showed efficient binding of PM to HSA an oxidative stress-related protein. Based on the results of in vitro, ex vivo, and in silico studies, further investigations are warranted in in vivo model to establish the cellular mechanism and pathway of PM to combat oxidative stress associated diseases like hepatotoxicity, diabetes, inflammation, apoptosis, cardiovascular, and neurological diseases.

ACKNOWLEDGMENTS

Financial support for this work was provided by the National Medicinal Plant Board (NMPB), Department of AYUSH, Govt. of India, New Delhi (Grant no. Z.18017/87/CSC/R&D/OR-01/2013-14-NMPB). We are also thankful to Sophisticated Analytical Instrumentation Facility (SAIF), Central Drug Research Institute (CDRI), Lucknow, India for providing NMR and Mass spectrometry study. FT-IR spectroscopy and HPTLC analysis were performed at Central Instrumentation Facility (CIF), Orissa University of Agriculture and Technology (OUAT), Bhubaneswar, Odisha.

CONFLICT OF INTEREST

The authors have declared no conflict of interest.

ORCID

Atish Kumar Sahoo
https://orcid.org/0000-0002-6524-4642

REFERENCES

1. Yuan, H., Ma, Q., Ye, L., Piao, G., The traditional medicine and modern medicine from natural products. *Molecules* 2016, *21*, 1–18.
2. Bruhn, J. G., Bohlin, L., Molecular pharmacognosy: an explanatory model. *Drug Discov. Today* 1997, *2*, 243–246.
3. Rao, J. K., Reddi, T. V. V. S., Kumar, O., Ethnobotany of stem bark of certain plants of Visakhapatnam district, Andhra Pradesh. *Curr. Biol.* 2011, *2*, 1–6.
4. Dhal, N. K., Panda, S. S., Muduli, S. D., Traditional uses of medicinal plants by native people in Nawarangpur district, Odisha, India. *Asian J. Plant Sci. Res.* 2015, *5*, 27–33.
5. Panda, S. K., Bastia, A. K., Sahoo, G., Process characteristics and nutritional evaluation of handia-a cereal based ethnic fermented food from Odisha. *Indian J. Tradit. Know.* 2014, *13*, 149–156.
6. Rao, J. K., Suneetha, J., Reddi, T. V. V. S., Kumar, O. A., Ethnomedicine of the Gadabas, a primitive tribe of Visakhapatnam district, Andhra Pradesh. *Int. Multidiscip. Res. J.* 2011, *1*, 10–14.
7. Mahapatra, A. K., Pani, S. S., Sahoo, A. K., Free radical-scavenging activities of *Homalium* species-an endangered medicinal plant of Eastern Ghats of India. *Nat. Prod. Res.* 2015, *29*, 2112–2116.
8. Kanhar, S., Sahoo, A. K., Mahapatra, A. K., The ameliorative effect of *Homalium nepalense* on carbon tetrachloride induced hepatocellular injury in rats. *Biomed. Pharmacother.* 2018, *103*, 903–914.
9. Gong, F., Wang, B. T., Chau, F. T., Liang, Y. Z., Data pre-processing for chromatographic fingerprint of herbal medicine with chemometric approaches. *Analytic. Letters* 2005, *38*, 2475–2492.
10. Khan, I., Sangwan, P. L., Dhar, J. K., Koul, S., Simultaneous quantification of five marker compounds of *Betula utilis* stem bark using a validated high-performance thin-layer chromatography method. *J. Sep. Sci.* 2012, *35*, 392–399.
11. Khatoon, S., Srivastava, M., Rawat, A. K. S., Mehrotra, S., HPTLC method for chemical standardization of *Sida* species and estimation of the alkaloid ephedrine. *J. Planar Chromat.* 2005, *18*, 364–;367.
12. Dash, U. C., Kanhar, S., Dixit, A., Dandapat, J., Sahoo, A. K., Isolation, identification, and quantification of pentylcurcumene from *Geophila repens*: a new class of cholinesterase inhibitor for Alzheimer's disease. *Bioorg. Chem.* 2019, *88*, 1–11.

13. Dar, A. A., Rath, S. K., Qaudri, A., Singh, B., Tasduq, S. A., Kumar, A., Sangwan, P. L., Isolation, cytotoxic evaluation, and simultaneous quantification of eight bioactive secondary metabolites from *Cicer microphyllum* by high-performance thin-layer chromatography. *J. Sep. Sci.* 2015, *38*, 4021–4028.
14. Tayade, N. G., Nagarsenker, M. S., Validated HPTLC method of analysis for artemether and its formulations. *J. Pharm. Biomed. Anal.* 2007, *43*, 839–844.
15. Morris, G. M., Huey, R., Lindstrom, W., AutoDock4 and AutoDockTools4: Automated docking with selective receptor flexibility. *J. Comput. Chem.* 2009, *30*, 2785–2791.
16. Trott, O., Olson, A. J., AutoDock Vina: improving the speed and accuracy of docking with a new scoring function, efficient optimization and multithreading. *J. Comput. Chem.* 2010, *31*, 455–461.
17. Henry, G. E., Momin, R. A., Nair, M. G., Dewitt, D. L., Antioxidant and cyclooxygenase activities of fatty acids found in food. *J. Agric. Food Chem.* 2002, *50*, 2231–2234.

SUPPORTING INFORMATION

Additional supporting information may be found online in the Supporting Information section at the end of the article.

How to cite this article: Kanhar S, Roy PP, Sahoo AK. Computational and experimental validation of free radical scavenging properties of high-performance thin-layer chromatography quantified phenyl myristate in *Homalium nepalense*. *J Sep Sci*. 2020;43:1566–1575. https://doi.org/10.1002/jssc.201901178